第15回性能に基づく橋梁等の耐震設計に関する
シンポジウム講演論文集（2012年7月）

Effect by Failure of Foundation on Deformation Behavior of a RC Rigid-Frame Arch Bridge Damaged in Wenchuan Earthquake

Zhongqi SHI[1],Kenji KOSA[2], Jiandong ZHANG[3], Tatsuo SASAKI[4]

[1]Ph.D. Candidate, Dept. of Civil Engineering, Kyushu Institute of Technology
(804-8550, Sensui 1-1,Tobata, Kitakyushu, Japan)
[2] Ph.D., Professor, Dept. of Civil Engineering, Kyushu Institute of Technology
(804-8550, Sensui 1-1,Tobata, Kitakyushu, Japan)
[3] Senior Engineer, Jiangsu Transportation Research Institute, China
(211112, Chengxin Road 2200, JiangningSciencePark, Nanjing, China)
[4]Manager, Technical Generalization Division, Nippon Engineering Consultants Co., Ltd.
(Currently in the doctoral program at Kyushu Institute of Technology)

1. INTRODUCTION

Wenchuan Earthquake occurred in Sichuan Province, China, at 2:28 p.m. on May 12th, 2008. It had the magnitude of 8.0 measured by CEA (China Earthquake Administration) and 7.9 by USGS (US Geographical Survey)[1]. Reports have been published saying that nearly 1600 bridges suffered extensive damage because of this great earthquake. Authors conducted a detailed field damage survey of Xiaoyudong Bridge on September 27th, 2009, (as the elevation drawing shown in **Fig. 1**) which crossed Baishui River in Xiaoyudong Town on Peng-Bai Road. This bridge is a 189m long, 13.6m wide, 4 spans, RC rigid-frame arch bridge that was built in 1998. Based on the study on the type of the rigid-frame arch bridge, it is a composite structural type of arch bridge and inclined rigid-frame bridge, and a higher-order hyperstatic structure with horizontal thrust, which has been abundantly constructed in China since 1980s[2]. According to the statistical investigation, the accumulative total span length of this light-weight type bridge is more than 15 thousands kilometers[2].

Previously, vibration characteristics of Xiaoyudong Bridge were studied briefly by 1-span model. However, the failure of pile beneath P3 was not taken into account. Besides, the deformation in the analysis could not able to reach the level observed in actual damage.

As illustrated in **Fig. 2**, aiming at examining the characteristics of seismic response in details and verifying the coincidence with actual damage, dynamic analysis is conducted considering the pile model beneath P3. Damage conditions of girder, legs and pile are summarized, as well as the deformation. Furthermore, comparison between actual damage and analytical result,

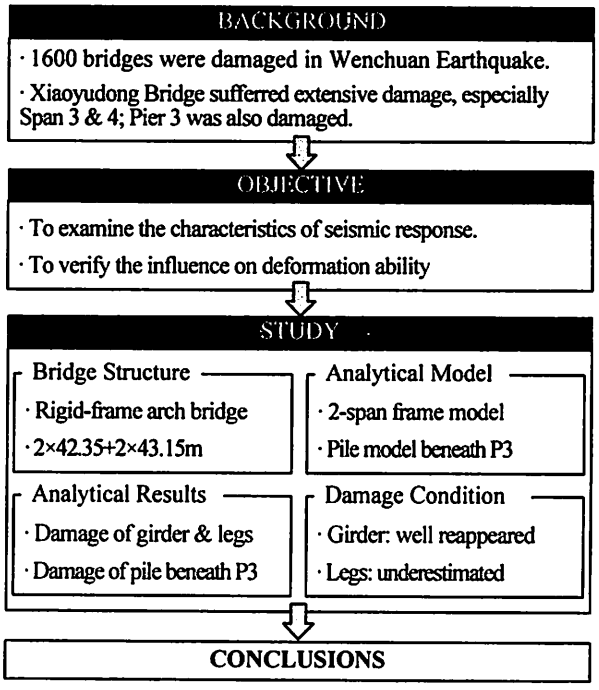

Fig. 2 Study Flow

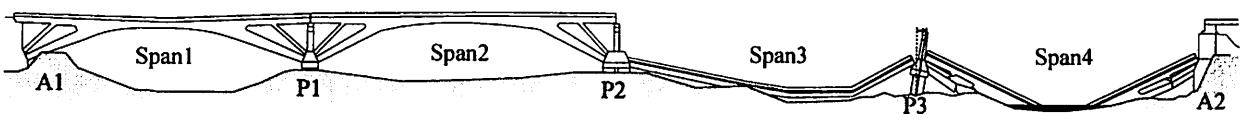

Fig. 1 General Damage Condition of Xiaoyudong Bridge (view from upstream)

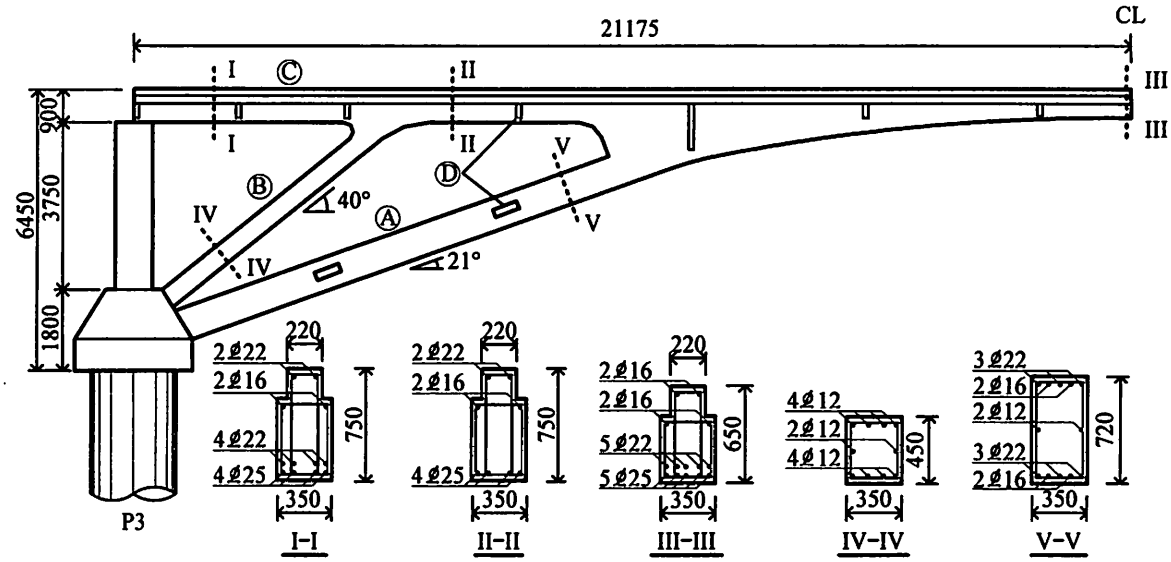

Fig. 3 Dimensions of Left Half Span of Span 4 (unit: mm)

based on which discussion about the reappearance is conducted.

2. Bridge Structure

Since the design drawings of Xiaoyudong Bridge are not available, the dimensions and the reinforcement condition have been assumed based on the results of field survey and referred from another RC rigid-frame arch bridge (Jinzhai No.6 Bridge[3]), Anhui Province, China), which has almost same characteristics as Xiaoyudong Bridge, for example the span length, the rise, the width-girder ratio and the design seismic fortification intensity of degree 7. As being illustrated in **Fig. 1**, all abutments, piers and spans were numbered from the left bank. According to the results measured by measuring tape, Span 1 has the length of 42.35m, while Span 2 and Span 3 have the same length of 43.15m. Thereby, considering the same length of Span 2 and Span 3, and no geographical limitation for piers and abutments, the bridge is considered symmetrical. Due to river went through Span 4, and the girder had collapsed into the water, it was impossible to measure the girder of Span 4. Thus the length of Span 4 was assumed as same as Span 1 of 42.35m, by noticing the symmetry of entire bridge.

The detailed dimensions of the left half span (P3 side) of Span 4 and P3 are respectively illustrated in **Fig. 3** and **Fig. 4** as examples. The arch leg (Point A in **Fig. 3**) and the inclined leg (Point B) has 21° and 40° slope for each and support the girder in the middle span. The arch frame is formed by two arch legs from pile caps on both sides, and the girder in the middle span. This arch frame, together with two inclined legs and the girder (Point C) at the ends, compose one single rigid-frame. One span consists of five rigid-frames connected by beams (Point D), arch slab (Point E in **Fig. 4**), and extending slab (Point F) in transverse direction. Then, four spans are supported by rubber bearings and connected by piers and abutments. A pier includes a reinforced concrete bending frame with two columns and abeam, upon which two

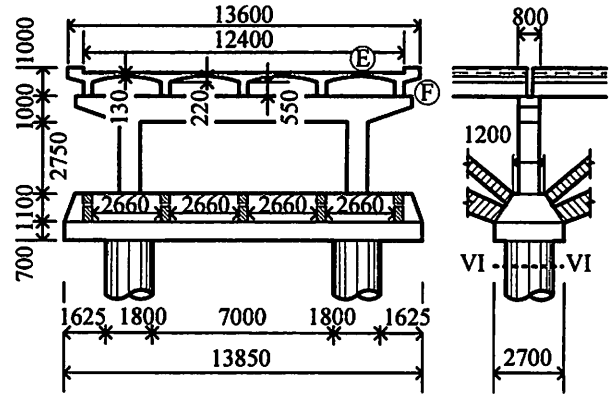

Fig. 4 Dimensions of P3 (unit: mm)

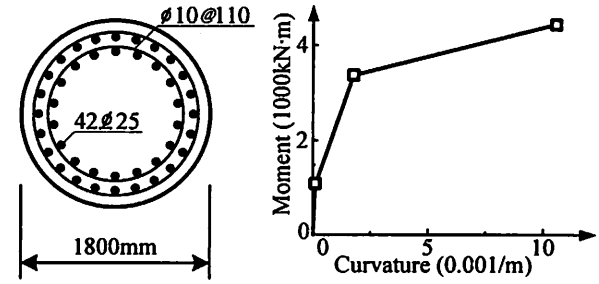

(a) VI-VI Section (b) M-Φ for VI-VI

Fig. 5 Cross Section of Pile beneath P3

decks are simply supported by rubber bearings. Legs are connected to pile cap, which is supported by RC piles.

Besides, by referring Jinzhai No.6 Bridge[3]) and using Chinese specifications as guideline, the detailed condition of reinforcement, including arrangements, numbers and diameters, has been assumed as shown as the cross sections in **Fig. 3**. As well, the concreteis set as C30 (standard compressive strength f_{ck}= 20.1N/mm^2). Main rebars are assumed as HRB335 (standard tensile strength f_{yk}= 335N/mm^2), and the area ratio is 0.72 % and 1.31 % for inclined legs and arch legs, and varies from 1.23 % to 2.27 % in the mid-span. Besides, stirrups are assumed as HPB235 (standard tensile strength f_{yk}= 235N/mm^2) and the area ratio is 0.076 %, 0.095 % and

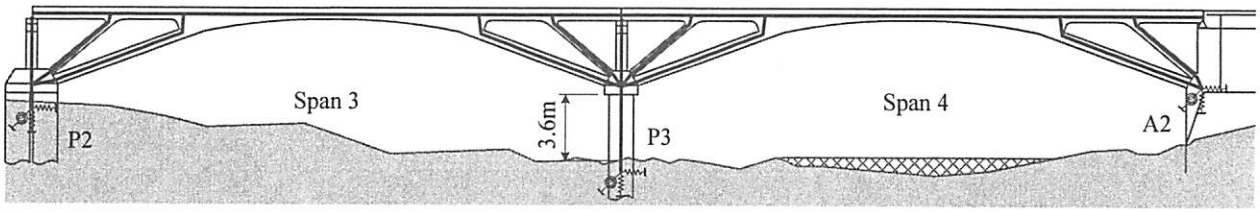

Fig. 6 Analytical Model (2-span) Considering Pile beneath P3

0.076 % for the inclined legs, arch legs and mid-span respectively.

Similarly, reinforcement for the pile beneath P3 (cross section VI-VI as shown in **Fig. 5** (a)) is assumed based on the sample as well. Consequently, the area ratio of main rebar is 0.83 % by HRB335 while the volume ratio of stirrups is 0.16 % by HPB235.

3. ANALYTICAL CONDITIONS

(1) Analytical Model

The model has been made for Span 3 &4 aiming at reappearing theiractual damage. As shown in **Fig. 6**, noticing five arch frames on the transversal direction of the axis, here select one single arch frame, including the slab, to establish the two dimensional model.

The pile beneath P3 has been exposed before the occurrence of Wenchuan Earthquake, which is a special character of Span 3 & 4 distinguished from Span 1 & 2. After the earthquake, about 7.5° residual tilt, and great damage were observed for P3and at bottom of pile near the ground surface respectively. Therefore, aiming at taking the damage of pile beneath P3 into consideration, tri-linear M-Φ model (as shown in **Fig. 5** (b)) is set for it, to simulate the exposure of it before the occurring of earthquake. Noticing relatively greater cross sectional area and greater amount of reinforcement, rigid elements have been set to the following parts: the footing, the beam on the top of the piers and the joints between legs and girder. Tri-linear M-Φ elements (here define yield stage of cross section as the tensile reinforcement reaches at standard tensile strength σ_y, and the ultimate stage of the cross section as the compressive concrete reaches at the ultimate strain of concrete ε'_u= 0.0035) calculated based on Japanese specifications are used for the other parts. Then, M-Φ relationships are calculated considering axial forces when only dead load acts on the structure.

Additionally, vertical, horizontal and rotational springs are utilized under P2, P3 and A2. For the springs between the girder and the pier, one frictional spring which is assumed to be comparatively weak, and one supporting spring are used on P3. On the other hand, the frictional and supporting springs are used on the top of A2 as same as that on P2 and P3. Currently, the collision spring on A2 is not taken into account.

(2) Seismic Wave

The response acceleration spectra, as shown in **Fig. 7**, are used to make comparison of the seismic wave by these two stations (since the direction of Xiaoyudong Bridge is approximately along East-West, thus E-W and U-D components of the response acceleration were compared). Compared with the standard seismic waves (Takatori wave) by Japanese specification, the seismic wave by Station B will probably affect more strongly on the structures with lower natural period. Seismic wave by Bajiao Station is used in the dynamic analysis. Both E-W and U-D components of the seismic waves, as shown in **Fig. 8**, are input. Therefore, the peak ground acceleration of +581gal occurred at 38.36s of the E-W component, and -633gal occurred at 37.40s of the U-D component.

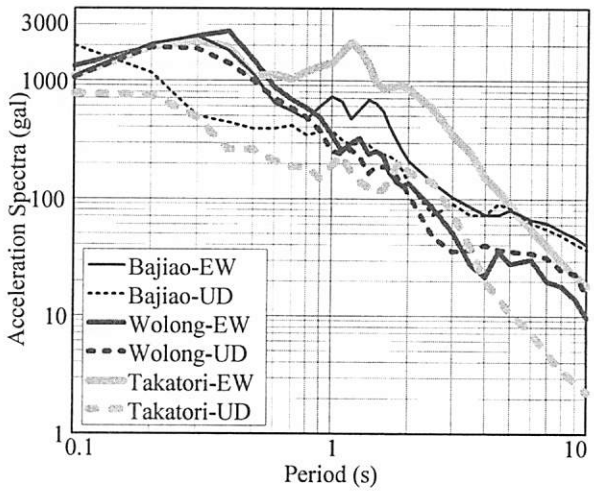

Fig. 7 Response Acceleration Spectra

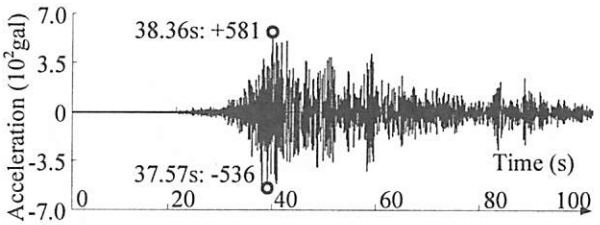

(a) E-W Component

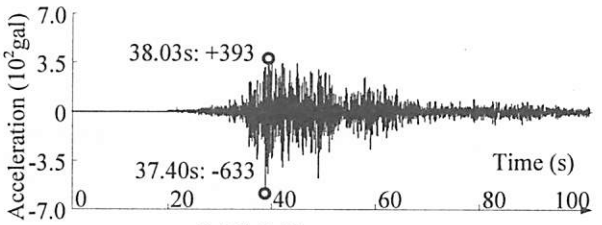

(b) U-D Component

Fig. 8 Seismic Wave by Bajiao Station

(3) Analytical Condition

Damping coefficient of 20 % and 2 % is separately utilized for the springs at bottom and all other elements. Rayleigh damping based on eigen-vibration analysis is applied for entire structure. The analysis starts from 0.0s and ends at 100.0s. For the calculation, Newmark-β (β=

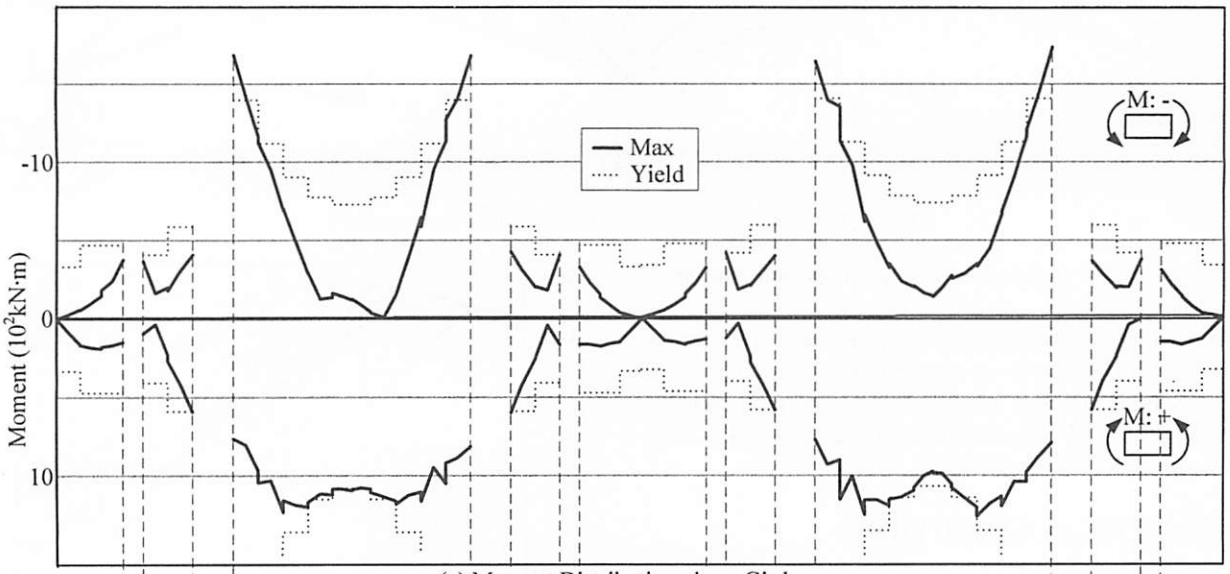

(a) Moment Distribution along Girders

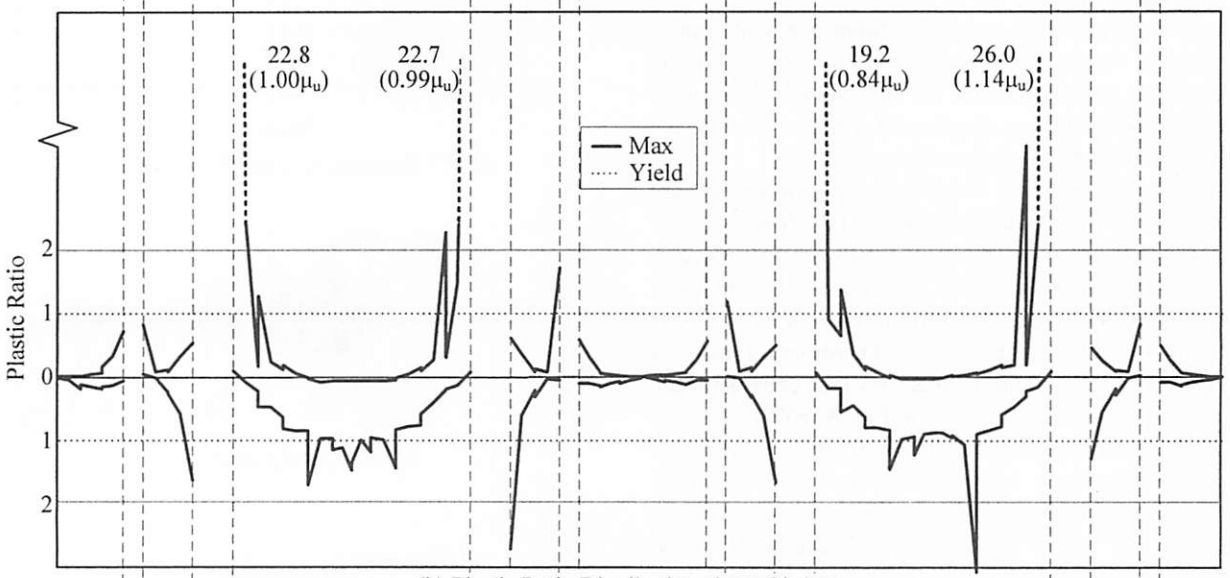

(b) Plastic Ratio Distribution along Girders

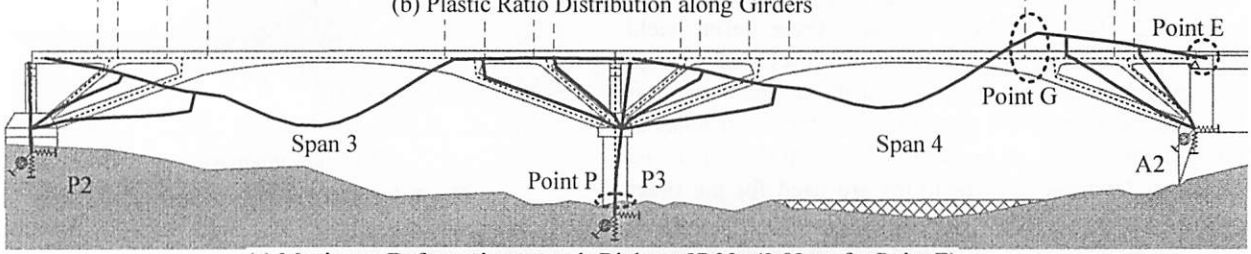

(c) Maximum Deformation towards Right at 57.32s (2.82cm for Point E)

Fig. 9 Maximum Flexural Response & Maximum Deformation

1/4) method is applied in the numerical integration with the time step being 1/1000s.

4. ANALYTICAL RESULTS

Being a rigid-frame arch bridge, flexural damage is the main failure type, which was also confirmed in the field survey. Therefore, the evaluations of analytical results are mainly divided into the flexural response and the deformation. Three observing points will be used in later discussion are defined as follows: Point G: right joint on Girder with arch leg on Span 4; Point P: bottom of Pile beneath P3; Point E: right End of girder on Span 4;

(1) Flexural Response

As the peak response moment distribution along the girder shown in **Fig. 9** (a), we can see that all elements of girder suffer changeable moment in both positive and negative direction. It should be noticed that the joint of girder with arch legs (for example the right joint on Span 4: Point G) are the most crucial point along girder, whose response moment exceeds the yield moment (defined by the yield of tensile reinforcement) and even the ultimate moment (defined by the compressive concrete reaches the ultimate strain ε_{cu}= 0.0035).

Furthermore, the maximum plastic ratio is also plotted in **Fig. 9** (b), defined by the equations as following:

$$\mu_{max} = \Phi_{max}/\Phi_y \quad (1)$$

where, μ_{max}: peak plastic ratio; Φ_{max} and Φ_y: peak response or yield curvature.

By Eq. 1, we got following phenomena: (1) all 4 joints with arch legs on Span 3 & 4 suffer most serious damage, whose maximum plastic ratios reach from 19.2 to 26.0 (Point G reached at 1.14 times of ultimate plastic ratio μ_u); (2)although other points, for instance the outside point of joints with arch legs and middle of both spans, receive relatively noticeable response as well, over yield stage, the absolute value of the maximum plastic ratio does not exceed 3.0 (smaller than $2\delta_y$ in experimental tests), therefore the failures at these points are limited.

Besides, from the M-Φ history of Point G, as shown in **Fig. 10**, we can see that opposite response acts on Point P from 42.01s, after several cyclic actions, maximum plastic ratio (26.0) is got at 57.32s

On the other hand, the pile beneath P3 is also damaged noticeably. The deformation at 57.32s (the time point when girder of Span 4 moves towards right most) of P3 is illustrated in **Fig. 11** (a), while the plastic ratio distributions at maximum and at 57.32s are shown in (b) together. It becomes obvious to us that significant slope change occurs around Point P seen from **Fig. 11** (a), this contributes the most to the tilt of P3 and 2.58cm on the top at 57.32s. The phenomenon is considered to be caused by relatively great response curvature (as plastic ratio being 0.82 at 57.32s) around Point P.

(2) Horizontal Deformation Behavior

To discuss the deformation behavior of this RC rigid-frame arch bridge, the plastic ratio histories for Point G and P are plotted in **Fig. 12** (a) and (b) respectively, while the accumulated maximum plastic ratio history (which can be considered as the representative for the development of residual flexural response) for Point G is shown in (a) together. From **Fig. 12** (a), three time points of sudden change of the accumulated maximum plastic ratio history can be discovered: ① for 36.60s, ② for 42.01s and ④ for 57.32s, respectively marked in **Fig. 10** as well. Besides, time point ③ is defined as 44.32s thanks to its maximum plastic ratio (μ_{max}= 1.22) of Point P as shown in **Fig. 12** (b). Therefore, at all these four representative time points, relatively noticeable variation ranges of plastic ratio can be observed for both Point G and P. It indicates that notable flexural response happens to these two points.

The displacement history of Point E (the right end of girder of Span 4) is shown in **Fig. 13**. Referring to four time points defined before, the horizontal displacement of Point E is got as 1.50cm, 2.00cm and 1.92cm for the first three, and maximum 2.82cm for time point ④.

Furthermore, the development of deformations for Span 4 for three representative time points ①, ② and ④ is illustrated in **Fig. 14**, for verifying the reason of different displacement with similarly noticeable flexural response. For the deformation at 36.60s shown in (a), P3 tilts and top of P3 moves towards right notably while the girder does not deform notably. Thus, the horizontal

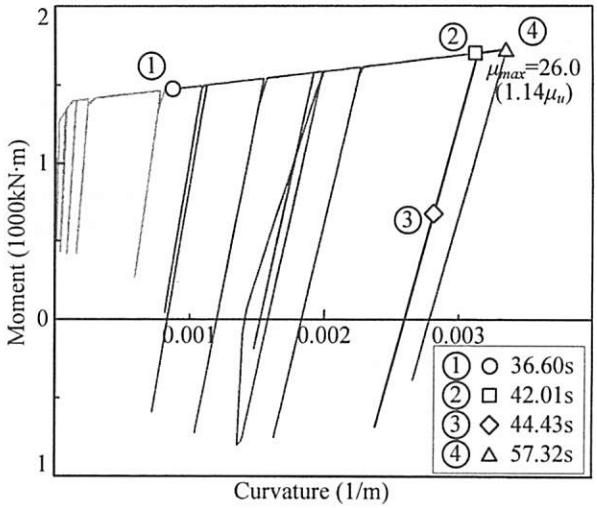

Fig. 10 M-Φ History of Point G (0.0s to 60.0s)

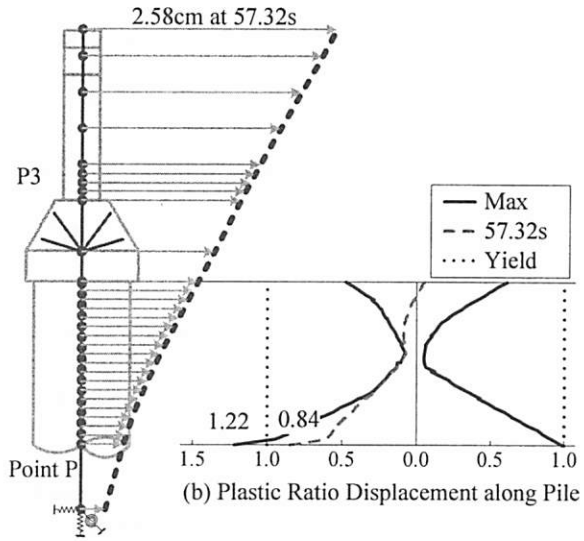

(a) Deformation of P3

(b) Plastic Ratio Displacement along Pile

Fig. 11 Response of P3 at 57.32s

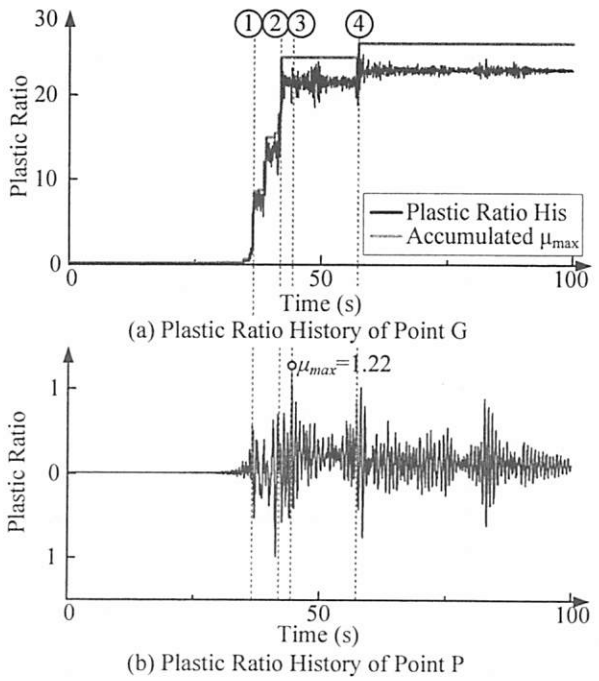

(a) Plastic Ratio History of Point G

(b) Plastic Ratio History of Point P

Fig. 12 Plastic Ratio Histories

displacement of Point E (1.50cm) is limited by the small deformation of girder. For the deformation at 42.01s shown in (b), the tilt of P3 is not great while the deformation of girder is significant. The displacement (2.00cm) is consequently not great as well. However, for deformation at 57.32s shown in (c), P3 and the girder of Span 4 vibrate harmoniously. Point P and G receive great flexural response, with the plastic ratio being 0.84 and 26.0 respectively, and both P3 and girder deform greatly from original position. Thus, the maximum horizontal displacement is got as 2.82cm at 57.32s.

(3) Summary

As the flexural response and the horizontal deformation ability being discussed above, following phenomena are found: (a) similar damage condition is got for Span 3 and Span 4, with the joints on the girder with arch legs suffering most severe failure, and the pile beneath P3 is damaged as well; (b) the deformation reaches its maximum value if only the girder and P3 vibrate together harmoniously, which suggests that without the damage of pile beneath P3, the horizontal displacement ability of this bridge will be weakened.

5. COMPARISON AND EVALUATION OF DAMAGE

Based on analytical result explained above, and actual damage condition according to detailed field survey, comparison is conducted to clarify the reappearance of this analysis and to confirm the damage of this bridge.

(1) Judgment of Actual Damage and Analytical Result

It should be explained for the damage judgment that by former study[4] on the damage of axial-loaded column, $1\delta_y$ stands for visible cracks in actual damage; $3\delta_y$ stands for single-side spalling of concrete, or exposure of main rebar, or great amount of cracks; $5\delta_y$ stands for plural-side spalling of concrete, or buckling of main rebars, or total loss of resistance in the actual damage. On the other hand, to coincide with the analytical result, relationship between δ_y and Φ_y are simply defined, as:

$$\begin{cases} n*\delta_y = n*\Phi_y & (n = 1) \\ n*\delta_y = (2\sim4)n*\Phi_y & (1 < n) \end{cases} \quad (2)$$

An example for the damage judgment at joints on girder with arch legs (Point f) of Span 2 is shown in **Fig. 15**. From this figure we can see that spalling of surface concrete occurred to the bottom, while the main rebar was exposed but no buckling was discovered. Thus, $3\delta_y$ can be defined.

(2) Comparison with Actual Damage of Span 3 & 4

As the damage condition is similar for Span 3 and Span 4 according to both the actual damage and the analytical result, comparison is going to be conducted for Span 3 as the representative.

The comparison results are listed in **Table. 1**, with the investigate point being illustrated in **Fig. 16**. Point a~d

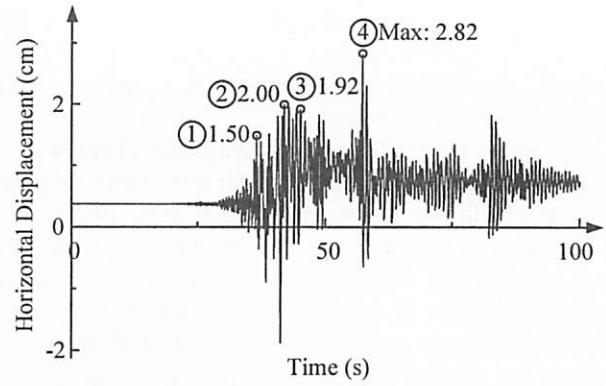

Fig. 13 Horizontal Displacement History of Point E

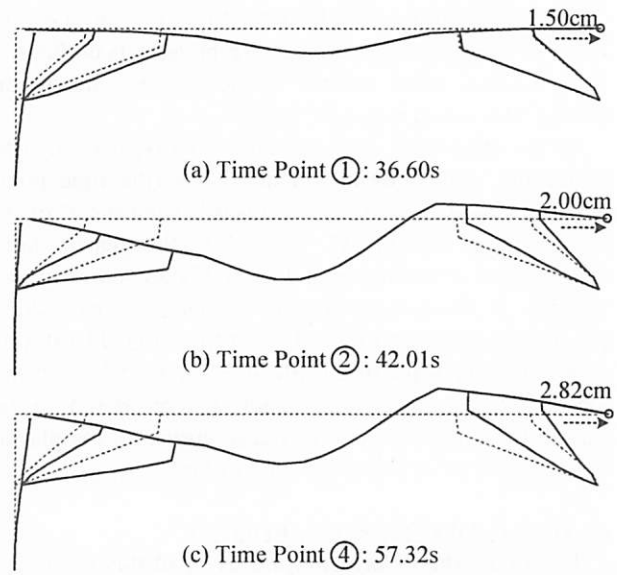

Fig. 14 Deformation Development of Span 4 (×50)

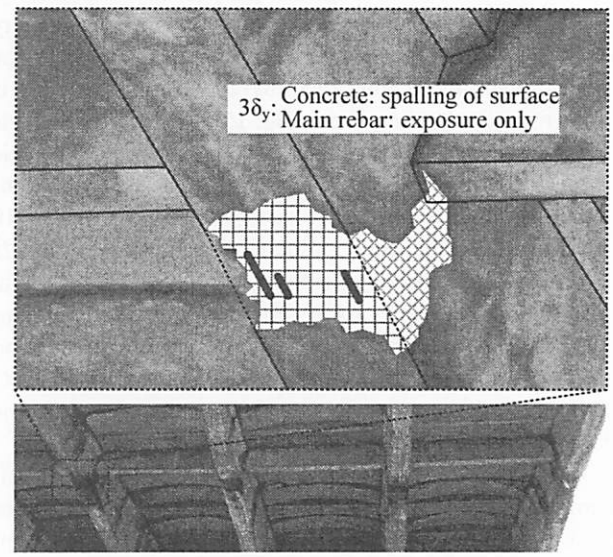

Fig. 15 Actual Damage of Point f of Span 2

and g~j are for the legs on left or right, while Point e and f are for the joints on girder with arch legs.

In the middle span of girder, near the joints with arch legs), actual damage is shown in **Fig. 17** for Pont f of Span 3. We can see cyclic load-induced cracks, spalling of concrete at both bottom and top, and buckling of

Table. 1 Summary of Comparison of Damage Condition between Actual Damage and Analytical Result

Point		ⓐ	ⓑ	ⓒ	ⓓ	ⓔ	ⓕ	ⓖ	ⓗ	ⓘ	ⓙ
Analytical Result		<1Φ_y				19.2~26.0Φ_y (0.84~1.14Φ_u)		<1Φ_y			
Actual Damage	Span 1	5δ_y	5δ_y	5δ_y	3δ_y	3δ_y		<1δ_y	<1δ_y	3δ_y	3δ_y
	Span 2	3δ_y	3δ_y	<1δ_y	<1δ_y	3δ_y		<1δ_y	<1δ_y	3δ_y	3δ_y
	Span 3	Complete failure		Failure after collapse of girder		5δ_y		Failure after collapse of girder		Complete failure	
	Span 4					5δ_y					

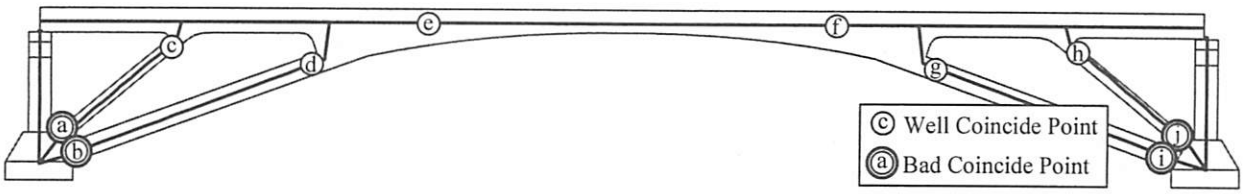

Fig. 16 Positions of Points in **Table. 1** (view from upstream)

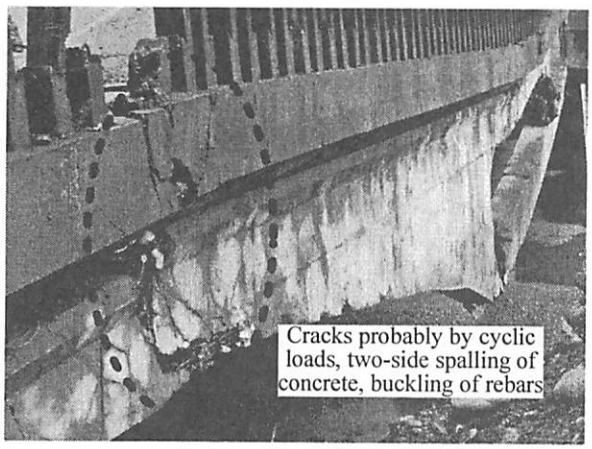

Fig. 17 Point f of Span 3

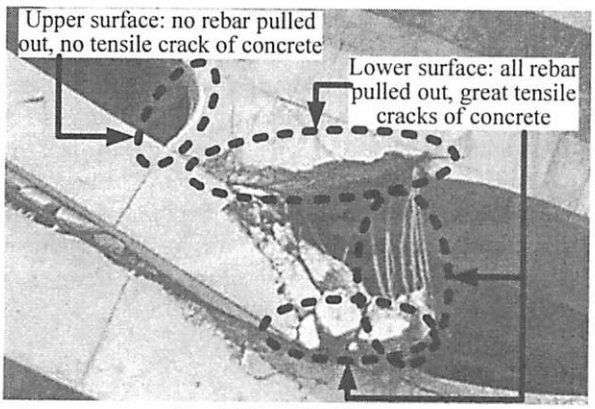

Fig. 18 Point h of Span 3

rebars. Thus, 5δ_y is judged for the actual damage. Furthermore, this 5δ_y damage is probably developed from the 3δ_y damage of Point f of Span 2 explained in **Fig. 15**, rather than totally damage by collapse, since the cyclic load-induced cracks. And shown in **Fig. 9**, 26.0 Φ_y or 1.14 Φ_u of Point G in analysis is got, which coincide with actual damage well. On the top of all legs (Point c, d, g and h, example is shown in **Fig. 18** for Point h of Span 3), neither pull-out rebar nor tensile crack of concrete was observed for upper surface, while all rebars were

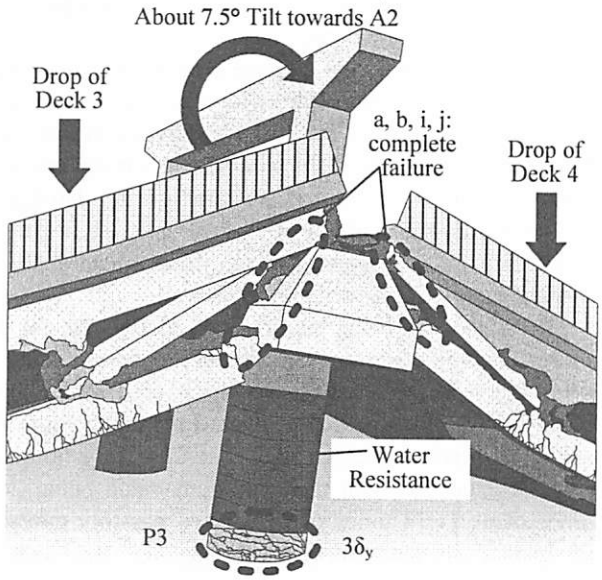

Fig. 19 Actual Damage of P3

pulled out and great tensile cracks occurred to concrete for lower surface. This indicates the damage is probably induced by collapse, rather than before it. At bottoms (Point a, b, i and j, **Fig. 19**) are damage completely. Thus, actual damage condition is not compared with analytical result for both tops and bottoms of all legs of Span 3 & 4. For P3, to the maximum, 2.58cm horizontal displacement on top and 1.22 Φ_y for pile in analysis is observed (about 1δ_y, illustrated formerly in **Fig. 11**), which is less severe than the residual 7.5° tilt towards A2 side and great amount of wide cracks in the actual damage by field survey (about 3δ_y, shown in **Fig. 19**).

(3) Comparison with Actual Damage of Span 1 & 2

During Wenchuan Earthquake, Span 1 & 2 stood still through this event, with the slightest damage among all 4 spans. Therefore, the damage condition of theirs is suitable to be considered as a preliminary step without extreme condition which may induce the entire collapse, of the damage development for other spans. On the other

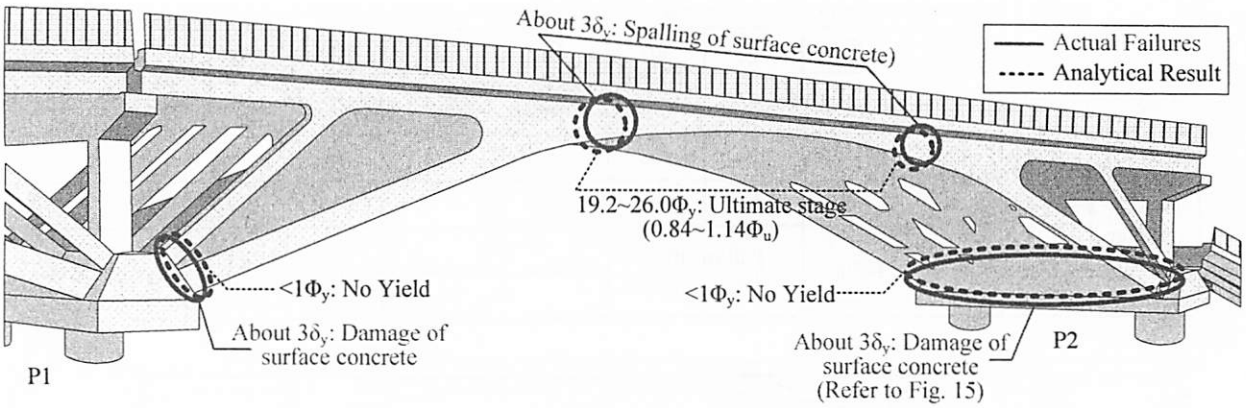

Fig. 20 Actual Damage Condition of Span 2 and Comparison with Analytical Result (view from upstream)

hand, although there is the able-to-tilt pile beneath P3 in Chapter 4 different from Span 1 & 2, analysis shows only 2.58cm displacement on the top of P3 for the maximum. Thus, comparison between actual damage and analytical result can be conducted for providing other evidence for the reappearance of damage.

For Span 1, the actual damage condition shows result of $3\delta_y$ for the joints on girder with arch leg. Therefore, it is slightly less severe than that by analytical result (26.0 Φ_y). For the legs, the right side shows similar result to Span 2. Bottoms of both legs suffered greater damage as $3\delta_y$ judged by the spalling of surface concrete in single-side and exposure of main rebars, than in the analysis, while the top coincide with analysis well.

For Span 2, as being summarized in **Fig. 20**, for the girder, spalling of surface concrete at the lower surface at the joints with arch legs were discovered in the field survey. Thus, about $3\delta_y$ is evaluated for them. From the analytical result explained above in Chapter 4, ultimate stage is exceeded with the maximum value being 26.0 times of Φ_y (1.14 times of Φ_u). Thus, possibly movable P3 in analysis leads more severe damage than that in actual at these joints. On the other hand, for bottoms of both arch legs and inclined legs on both sides, $3\delta_y$ is estimated. However, analytical result shows relatively slight damage for these points without any yield observed. This contrast suggests, by the dynamic analysis using Bajiao wave, the response of legs is underestimated, comparing with the actual damage condition.

(4) Discussion

To sum it up, the damage of girder is estimated well in the analysis, as 19.2~26.0 Φ_y is got in the analysis comparing with the damage of 3~5 δ_y in actual damage, and it is mainly caused by the cyclic load from seismic effect. On the other hand, as Point a, b, i and j being highlighted in **Fig. 16**, the damage at the bottoms of inclined legs and arch legs is underestimated in analysis. For bottoms of legs of Span 2 and on right side of Span 1, analysis still shows less notable damage without extreme condition. Besides, deformation of Span 3 and 4 is also less currently, which leads to no collapse of girder. Possible reasons and solutions for these underestimation include:

a) Model of the concrete truss structure formed by arch leg, inclined leg and girder is too strong in current analysis. Since assumption based on similar bridge is applied at present, there is necessity to clarify actual reinforcement arrangement.

b) Moderate wave form (from Bajiao Station) by Wenchuan Earthquake is applied in current dynamic analysis. However, the soil condition is also different for these two spots. As shown in **Fig. 7**, Wolong wave is also possible to be used although too far from the bridge. The wave form at the just-point or suitable wave form should be studied in the future.

6. CONCLUSIONS

Based on the dynamic analysis for Xiaoyudong Bridge, and the comparison with actual damage condition based on field survey, following conclusions have been drawn:

(1) Based on the analytical result, joints on girder with arch legs suffer most severe failure (even beyond ultimate stage), and pile beneath P3 is also damaged. They are crucial points for this type of bridge.

(2) By the analysis as well, deformation reaches its maximum value (2.82cm) if only P3 and girder vibrate together harmoniously, which suggests that without the damage of pile beneath P3, the horizontal displacement ability of this bridge will be weakened.

(3) By the comparison between actual damage condition and analytical result, actual damage is roughly well reappeared for girder with acceptable accuracy, but relatively underestimated for pile and legs.

REFERENCES

1) Kawashima, K. et al: Damage of Bridges in 2008 Wenchuan Earthquake, Investigation Report on the 2008 Wenchuan Earthquake, China, Grant-in-Aid for Special Purposes of 2008, MEXT, No. 20900002, 2009

2) Ren, H. et al: Inspection and Design Suggestion on Rigid-FrameArchBridge, the 1st Chinese-Croatian Joint Colloquium on Long Arch Bridge, pp. 309-315, 2008

3) Anhui Communications Consulting & Design Institute: Design Drawings and Construction Illustration of Jinzhai No.6 Bridge, 2002

4) Kosa, K. et al: Evaluation of Earthquake-Damaged RC Piers by the Ultimate Bearing Capacity Procedures, Journal of JSCE, No. 592/V-39, pp. 73-82, 1998